

## Unique Electronic and Structural Properties of 1,4-Benzoquinones: Crystallochemistry of Alkali Chloranilate Hydrates\*

Krešimir Molčanov,<sup>a</sup> Biserka Kojić-Prodić,<sup>a,\*\*</sup> and Anton Meden<sup>b</sup>

<sup>a</sup>Ruđer Bošković Institute, P. O. Box 180, 10002 Zagreb, Croatia

<sup>b</sup>Faculty of Chemistry and Chemical Technology, University of Ljubljana, Slovenia

RECEIVED SEPTEMBER 24, 2008; REVISED FEBRUARY 13, 2009; ACCEPTED APRIL 9, 2009

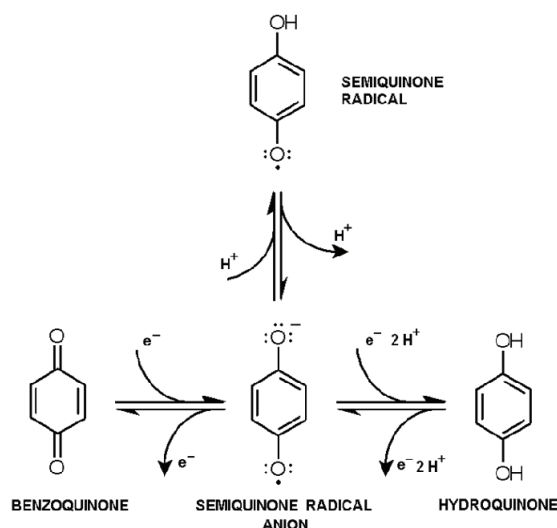
**Abstract.** The unique electronic and structural characteristics of 1,4-benzoquinones with possibilities for numerous interactions such as coordination, hydrogen bonding accompanied by proton and/or electron transfer,  $\pi$ -interactions, and redox activity, are used by nature to perform important biological reactions. In spite of their wide use in supramolecular chemistry for construction of functional materials, the intercorrelation of their versatile interactions has not been completely evaluated. The impacts of hydrogen bonding and cations on interactions of quinoid skeleton are studied on the prepared series of alkali ( $\text{Li}^+$ ,  $\text{Na}^+$ ,  $\text{K}^+$ ,  $\text{NH}_4^+$ , and  $\text{Rb}^+$ ) chloranilate hydrates, and anhydrous caesium homologue. The  $\pi\cdots\pi$  stacking interactions of chloranilate dianions observed in the structures of sodium chloranilate dihydrate and caesium sodium chloranilate monohydrate [with centroid separation distances of 3.662(1) and 3.740(2) Å and shifts of 1.698 and 1.358 Å, respectively] are tuned by hydrogen bonding involving water molecules. The crystal structures of potassium and rubidium chloranilate monohydrates are isostructural whereas their ammonium homologue, due to the presence of cation with pronounced proton-donor activity, exhibits completely different hydrogen bonding network. In the six of seven structures studied chloranilate dianion reveals the crystallographic symmetry  $C_i$ .

**Keywords:** 1,4-benzoquinones, chloranilic acid and derivatives, electronic properties, structural properties, hydrogen bonds,  $\pi$ -stacking, crystallochemistry of alkali chloranilate hydrates

### INTRODUCTION

The chemistry of quinones is a very broad field of research due to specific electronic structure and properties. Some of the examples given in this introduction illustrate how deep knowledge on quinone chemistry is required in everyday life and also in bioinspired synthesis based on quinones. The electronic properties and structural characteristics of 1,4-benzoquinones are responsible for variety of donor and acceptor functions that can be accompanied by a proton transfer coupled with an electron transfer<sup>1,2</sup> (Scheme 1).

The substitutions of electron withdrawing groups such as  $-\text{NO}_2$ ,  $-\text{CN}$ , or  $-\text{COOH}$  raise the oxidation potential making quinones more powerful oxidants whereas the electron donating substitutions using  $-\text{OCH}_3$ ,  $-\text{CH}_3$ ,  $-\text{OH}$ ,  $-\text{NH}_2$ ,  $-\text{C}_6\text{H}_5$  lower the oxidation potential. A potent oxido/reduction property makes the system widely used by nature in living organisms for bioenergetic processes such as respiration and photosyn-



**Scheme 1.** Mechanism of the redox reactions in the quinone/hydroquinone system.

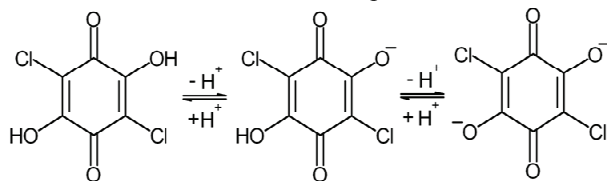
\* Dedicated to Professor Emeritus Drago Grdenić, Fellow of the Croatian Academy of Sciences and Arts, on the occasion of his 90<sup>th</sup> birthday.

\*\* Author to whom correspondence should be addressed. (E-mail: kojic@irb.hr)

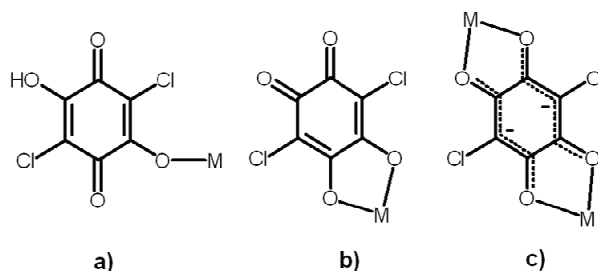
thesis but also in electrochemistry,<sup>3</sup> analytical chemistry<sup>4</sup> of a broad application, paper industry, recovery of precious metals (silver, gold, palladium, and platinum) and many more reactions. In many biological systems semiquinone radical intermediates were detected.<sup>5</sup> Electrochemical studies of reduction products of quinones, mainly semiquinone radical anions and hydroquinones, revealed that their stability and reactivity depend on hydrogen bonding and protonation.<sup>6</sup> An impact of hydrogen bonding interactions on the electronic structure of semiquinone studied by EPR spectroscopy and validation of experimental results by density functional methods was already demonstrated for biologically relevant quinones.<sup>7</sup>

Astrobiologists from Astrobiology Analytical Laboratory of NASA reconstructed conditions of interstellar space in a laboratory to imitate syntheses of compounds essential for living organisms such as quinones, amino acids, and amphiphiles.<sup>8</sup> Their results add a new view on the origin of life that might have emerged not from some warm primordial slime on Earth, but in the icy heart of space. They also demonstrated that complex molecules essential for life on Earth today can be produced in the conditions of interstellar space. New evidences of enzymes working with quinones as a prosthetic groups or substrates and understanding of their mechanisms will demonstrate how simple quinone molecule can exhibit very complex chemical reactions responsible for respiration, photosynthesis, and many protective mechanisms against radicals. Coenzyme Q, the ubiquinone, is present in animals, plants and microorganisms, and it is involved in electron transfer in photosynthesis, oxidative phosphorylation, the bioactivity of vitamin K, and many others.<sup>9</sup>

Many cellular oxidoreductases participate in metabolism of quinone compounds catalyzing one or two-electron reduction, as for example, cytochrome P450 reductase. The resultant semiquinone species are readily oxidized by O<sub>2</sub> with accompanied production of a harmful superoxide radical. However, cytosolic mammalian quinone oxidoreductases (QR1 and QR2) catalyse two-electron reduction of quinones producing dihydroquinones which are glucuronidated and rapidly excreted. Their metabolism does not include production of harmful semiquinone and oxygen species that can damage the cells. Thus, two-electron reduction of quinones seems to be a fundamental protective mechanism



**Scheme 2.** Dissociation of chloranilic acid.



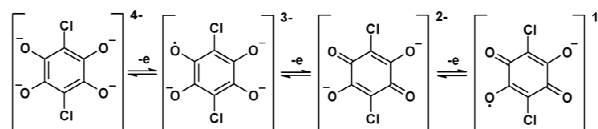
**Scheme 3.** The forms of chloranilate anion functioning as a ligand in transition metal complexes: a) *p*-quinone, b) *o*-quinone, and c) bis-carbanion.

in mammals.<sup>10</sup> There is also an important aspect of quinones related to mechanisms of polyphenol oxidases (PPO).<sup>11</sup> These enzymes catalyse oxidation of phenolic compounds to quinones (both, *ortho*- and *para*-Q); oxidative browning reactions proceed in food of plant origin, mainly causing deterioration on food quality by changing nutritional and organoleptic value. Browning reactions occur due to chemical reactions of highly active quinones with amino acids of plant proteins.<sup>12</sup> In production of champagne these reactions are used under control to reach better taste, bouquet, sparkle and foam. Enzyme browning in processing of black tea, coffee, and cocoa is beneficial to some extent as it enhances the quality of the beverages.

The chloranilic acid, 2,5-dichloro-3,6-dihydroxy-1,4-benzoquinone (H<sub>2</sub>CA) is a member of a broad class of 3,6-dihydroxy-benzoquinones with a general formula H<sub>2</sub>C<sub>6</sub>X<sub>2</sub>O<sub>4</sub> where X can be H or any other electron withdrawing or donating substituent that modifies the electronic structure and properties of the system. These properties make them attractive for studying hydrogen bonding including proton transfer and charge transfer complexes. Chloranilic acid, H<sub>2</sub>C<sub>6</sub>Cl<sub>2</sub>O<sub>4</sub>, the strong acid (pK<sub>a1</sub> = 0.76; pK<sub>a2</sub> = 3.08), dissociates into mono- (HCA<sup>-</sup>) and dianion (CA<sup>2-</sup>) (Scheme 2) and can be used for the preparation of metal complexes<sup>13–18</sup> (Scheme 3), salts, proton transfer, and charge transfer complexes.<sup>19–23</sup>

The dianions [C<sub>6</sub>X<sub>2</sub>O<sub>4</sub>]<sup>2-</sup> undergo one-electron oxidation and two one-electron reduction processes generating species with charges from -4 to -1 (Scheme 4) where the species with -1 and -3 are radicals.<sup>24,25</sup>

The electronic property can be also used in the synthesis of binuclear complexes of transition metals bridged by this type of ligand; such complexes can



**Scheme 4.** Four possible oxidation states of chloranilic acid.

include various valence states of the metal and/or ligand sites resulting in different spin states achieving molecular magnets.<sup>24</sup>

As summarised by Kitagawa and Kawata,<sup>16</sup> dihydroxybenzoquinone dianion and its derivatives are unique multifunctional ligands involving versatile interactions such as coordination, hydrogen bonding, ionic interactions,  $\pi$ -interactions, and also strong redox activity. The characteristics of this system direct its use in supramolecular chemistry and crystal engineering. In the synthesis of metal complexes these molecules can produce various coordination modes generating the networks of different topologies involving one-dimensional, two-dimensional and three-dimensional motifs useful for synthesis of functional materials.<sup>26–31</sup> Interactions with transition metal orbitals can be predicted and used in design of functional materials (*e.g.* molecular magnets).<sup>24</sup> However, interactions in the solid state with alkali metals have been less studied and their interactions hardly can be forecast. Nonaromatic chloranilate anions with their  $\pi$ -electrons are subjected to strong  $\pi$ -interactions influenced by hydrogen bonding.<sup>7,32,33</sup> Therefore, a series of alkali chloranilates hydrates was prepared and their structures analysed in order to evaluate polarization effects of hydrogen bonds and cations on the crystal packing of chloranilates.

## EXPERIMENTAL

Anhydrous caesium chloranilate and sodium chloranilate dihydrate were prepared by evaporation of absolute

ethanolic solution in a dry environment. All other compounds were prepared by evaporation of aqueous or ethanolic solutions of chloranilic acid (freshly prepared by Gräbe's method<sup>34</sup>) and equimolar amount of the corresponding base(s), at room temperature. Alkali carbonates and 25 % aqueous ammonia (Kemika, p.a. grade) were used.

Majority of crystallization samples were heterogeneous and crystals used for data collection were selected under stereomicroscope.

All crystallographic measurements were done at room temperature. Data reduction was performed by programs XCAD4<sup>35</sup> (CAD-4), CrysAlis PRO<sup>36</sup> (Xcalibur Nova) and DENZO and SCALEPACK<sup>37</sup> (Kappa CCD). Three standard reflections were measured every 120 minutes as intensity control for structures measured on the CAD-4 diffractometer. The structures were solved with SHELXS97<sup>38</sup> and refined with SHELXL97.<sup>38</sup> The models were refined using the full matrix least squares refinement with all non-hydrogen atoms refined anisotropically. Hydrogen atoms were located from difference Fourier maps and refined with the following restraints (using DFIX and DANG commands in SHELXL97<sup>38</sup>):  $d(\text{O}_{\text{water}}-\text{H}) = 0.95(2)$  Å,  $d(\text{N}_{\text{ammonium}}-\text{H}) = 0.85(2)$  Å; bond angles in water molecules and ammonium ions were constrained with  $d(\text{H}\cdots\text{H}) = 1.50(4)$  Å. The atomic scattering factors were those included in SHELXL97.<sup>38</sup> Molecular geometry calculations were performed with PLATON98,<sup>39</sup> molecular graphics were prepared using ORTEP-3,<sup>40</sup> and CCDC-Mercury.<sup>41</sup> Crystallographic and refinement data for the reported structures are shown in Table 1.

**Table 1.** Crystallographic data and details of data collection and structure refinement data

Compound	Li <sub>2</sub> CA · H <sub>2</sub> O	Na <sub>2</sub> CA · 2H <sub>2</sub> O	K <sub>2</sub> CA · H <sub>2</sub> O	(NH <sub>4</sub> ) <sub>2</sub> CA · H <sub>2</sub> O
Empirical formula	C <sub>6</sub> H <sub>2</sub> Cl <sub>2</sub> Li <sub>2</sub> O <sub>5</sub>	C <sub>6</sub> H <sub>4</sub> Cl <sub>2</sub> Na <sub>2</sub> O <sub>6</sub>	C <sub>6</sub> H <sub>2</sub> Cl <sub>2</sub> K <sub>2</sub> O <sub>5</sub>	C <sub>6</sub> H <sub>10</sub> Cl <sub>2</sub> N <sub>2</sub> O <sub>5</sub>
Molar mass / g mol <sup>-1</sup>	238.86	288.98	303.18	261.06
Crystal dimensions / mm	0.15 × 0.11 × 0.06	0.30 × 0.18 × 0.12	0.28 × 0.10 × 0.08	0.30 × 0.10 × 0.07
Space group	C2/c	P2 <sub>1</sub> /n	C2/c	C2/c
<i>a</i> / Å	12.8739(5)	8.9167(4)	16.1492(14)	16.981(2)
<i>b</i> / Å	13.9513(3)	3.6621(2)	4.8131(6)	4.7750(6)
<i>c</i> / Å	7.0192(3)	14.6030(7)	13.7472(12)	14.0935(13)
$\alpha$ / °	90	90	90	90
$\beta$ / °	138.556(3)	97.049(4)	117.320(7)	118.013(7)
$\gamma$ / °	90	90	90	90
<i>Z</i>	4	2	4	4
<i>V</i> / Å <sup>3</sup>	834.44(7)	473.24(4)	949.35(17)	1008.9(2)
<i>D</i> <sub>calc</sub> / g cm <sup>-3</sup>	1.901	2.028	2.121	1.719
Diffractometer type	Oxford Diffraction Xcalibur Nova	Oxford Diffraction Xcalibur Nova	Enraf-Nonius CAD-4	Enraf-Nonius CAD-4
Radiation	CuK $\alpha$	CuK $\alpha$	CuK $\alpha$	CuK $\alpha$

CA = chloranilate dianion [C<sub>6</sub>O<sub>4</sub>Cl<sub>2</sub>]<sup>2-</sup>

(continued)

**Table 1.** Crystallographic data and details of data collection and structure refinement data (continued)

Compound	Li <sub>2</sub> CA·H <sub>2</sub> O	Na <sub>2</sub> CA·2H <sub>2</sub> O	K <sub>2</sub> CA·H <sub>2</sub> O	(NH <sub>4</sub> ) <sub>2</sub> CA·H <sub>2</sub> O
$\lambda / \text{\AA}$	1.54184	1.54184	1.54184	1.54184
$\mu / \text{mm}^{-1}$	6.976	7.238	14.048	5.904
Absorption correction	multi-scan	multi-scan	psi-scan	psi-scan
$T_{\min}, T_{\max}$	0.4034, 0.6600	0.4631; 1.0000	0.1618; 0.3187	0.5259; 0.6575
$\theta$ range / °	6.09–75.9	5.53–75.61	6.17–75.89	5.9–76.04
Range of $h, k, l$	–14 < $h$ < 16; –17 < $k$ < 13; –8 < $l$ < 8	–10 < $h$ < 10; –4 < $k$ < 3; –18 < $l$ < 18	–18 < $h$ < 20; –6 < $k$ < 0; –17 < $l$ < 0	–10 < $h$ < 10; –4 < $k$ < 3; –18 < $l$ < 18
Reflections collected	2214	2461	1031	2086
Independent reflections	841	969	985	1047
Observed reflections ( $I \geq 2\sigma$ )	812	947	869	925
$R_{\text{int}}$	0.0175	0.0155	0.0854	0.0391
$R (F)$	0.0325	0.0432	0.0373	0.0253
$R_w (F^2)$	0.0917	0.1195	0.1058	0.0718
Goodness of fit	1.161	1.178	1.091	1.051
No. of parameters	74	81	74	90
$\Delta\rho_{\text{max,min}} / \text{e}\text{\AA}^{-3}$	0.353, –0.345	0.645, –0.224	0.691, –0.471	0.287, –0.182

Compound	Rb <sub>2</sub> CA·H <sub>2</sub> O	Cs <sub>2</sub> CA	Cs <sub>1.5</sub> Na <sub>0.5</sub> CA·H <sub>2</sub> O
Empirical formula	C <sub>6</sub> H <sub>2</sub> Cl <sub>2</sub> Rb <sub>2</sub> O <sub>5</sub>	C <sub>6</sub> Cl <sub>2</sub> O <sub>4</sub> Cs <sub>2</sub>	C <sub>6</sub> H <sub>2</sub> Cl <sub>2</sub> Cs <sub>1.5</sub> Na <sub>0.5</sub> O <sub>5</sub>
Molar mass / g mol <sup>–1</sup>	395.92	472.78	435.84
Crystal dimensions / mm	0.20 × 0.16 × 0.12	0.20 × 0.08 × 0.04	0.20 × 0.20 × 0.16
Space group	<i>C2/c</i>	<i>P2<sub>1</sub>/c</i>	<i>C2/c</i>
$a / \text{\AA}$	16.8277(5)	5.1890(1)	15.8241(4)
$b / \text{\AA}$	4.94390(10)	11.4219(4)	11.5237(3)
$c / \text{\AA}$	13.6609(5)	8.3424(2)	11.5179(2)
$\alpha / ^\circ$	90	90	90
$\beta / ^\circ$	117.337(2)	93.907(2)	101.248(1)
$\gamma / ^\circ$	90	90	90
$Z$	4	2	8
$V / \text{\AA}^3$	1009.59(5)	493.29(2)	2059.97(8)
$D_{\text{calc}} / \text{g cm}^{-3}$	2.605	3.183	2.811
Diffractometer type	Nonius Kappa CCD	Nonius Kappa CCD	Nonius Kappa CCD
Radiation	MoK $\alpha$	MoK $\alpha$	MoK $\alpha$
$\lambda / \text{\AA}$	0.71073	0.71073	0.71073
$\mu / \text{mm}^{-1}$	10.218	7.912	5.871
Absorption correction	Multi-scan	Multi-scan	Multi-scan
$T_{\min}, T_{\max}$	0.153, 0.293	0.370, 0.730	0.294, 0.391
$\theta$ range / °	4.34–27.41	3.57–27.45	2.62–27.52
Range of $h, k, l$	–21 < $h$ < 21; –6 < $k$ < 5; –17 < $l$ < 17	–6 < $h$ < 6; –14 < $k$ < 13; –10 < $l$ < 10	–20 < $h$ < 20; –14 < $k$ < 14; –14 < $l$ < 14
Reflections collected	1982	1956	4379
Independent reflections	1153	1120	2359
Observed reflections ( $I \geq 2\sigma$ )	1063	1021	2190

CA = chloranilate dianion [C<sub>6</sub>O<sub>4</sub>Cl<sub>2</sub>]<sup>2–</sup>

(continued)

**Table 1.** Crystallographic data and details of data collection and structure refinement data (continued)

Compound	Rb <sub>2</sub> CA·H <sub>2</sub> O	Cs <sub>2</sub> CA	Cs <sub>1.5</sub> Na <sub>0.5</sub> CA·H <sub>2</sub> O
$R_{\text{int}}$	0.0207	0.0133	0.0167
$R(F)$	0.0252	0.0177	0.0255
$R_w(F^2)$	0.0639	0.041	0.1029
Goodness of fit	1.072	1.136	1.266
No. of parameters	74	64	146
$\Delta\rho_{\text{max,min}} / \text{e}\text{\AA}^{-3}$	0.447, -0.556	0.366, -0.584	1.215, -1.133

CA = chloranilate dianion [C<sub>6</sub>O<sub>4</sub>Cl<sub>2</sub>]<sup>2-</sup>

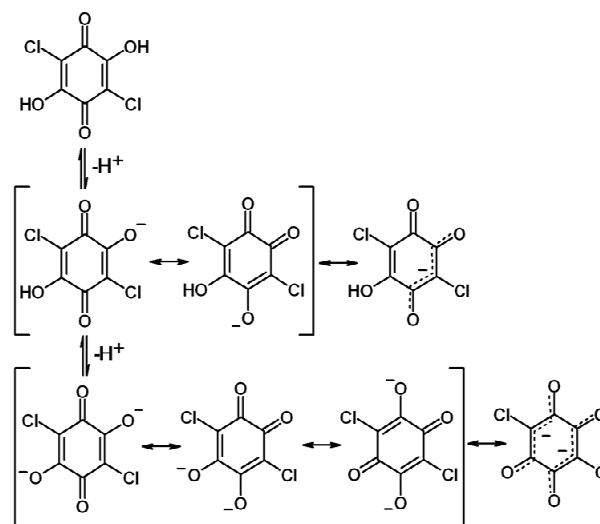
## RESULTS AND DISCUSSION

### Crystallochemistry of Alkali Chloranilates Hydrates

According to Herbstein & Kaftory<sup>15</sup> using X-ray film data (unit cells and space groups were reported, only) and Anderson's structure analysis<sup>14</sup> ammonium, potassium and rubidium chloranilates monohydrates are isostructural, belonging to the space group *C2/c*. Here, we report crystal structures of M<sub>2</sub>(C<sub>6</sub>Cl<sub>2</sub>O<sub>4</sub>)·H<sub>2</sub>O where M = Li<sup>+</sup>, NH<sub>4</sub><sup>+</sup>, K<sup>+</sup>, and Rb<sup>+</sup>. The structure of ammonium chloranilate monohydrate was first solved in 1967 by Andersen<sup>14</sup> using film data; here we present the more accurate structure with located protons. The analogous Cs<sup>+</sup> chloranilate monohydrate, reported by Herbstein & Kaftory,<sup>15</sup> after several crystallization attempts was not obtained. However, crystals of anhydrous salt were obtained in a dry atmosphere from an absolute ethanol and its structure is presented here. During crystallization from aqueous solution, only a few single crystals of a caesium salt Cs<sub>1.5</sub>Na<sub>0.5</sub>CA·H<sub>2</sub>O, were formed due to a presence of a small amount of NaCl. A novel salt of sodium chloranilate dihydrate, reported here, was crystallised from ethanol with traces of water originating from neutralisation of the acid with sodium carbonate whereas crystallization from aqueous solution yielded the well-described Na<sub>2</sub>(C<sub>6</sub>Cl<sub>2</sub>O<sub>4</sub>)·3H<sub>2</sub>O.<sup>15,42</sup>

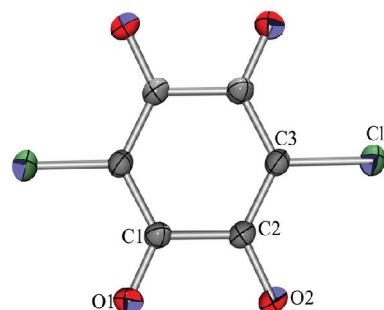
### Electron and Structural Characteristics of Chloranilate Dianion

According to the resonance (Scheme 5), chloranilate dianion has a *D<sub>2h</sub>* molecular symmetry. An inspection of the CSD<sup>13</sup> for homologous structures revealed that dianion centroid is located in the crystallographic inversion centre with the molecular symmetry *C<sub>i</sub>* in the majority of structures found. Among the seven structures reported here, six have a dianion of the *C<sub>i</sub>* symmetry, while the centrosymmetric structure of Cs<sub>1.5</sub>Na<sub>0.5</sub>CA·H<sub>2</sub>O is an exception having a dianion of no crystallographic symmetry. The chloranilate dianion consists of two separate resonance systems with delocalised  $\pi$  electrons; these two systems are separated by two single C–C bonds (Scheme 5). The four delocalised C–C

**Scheme 5.** Dissociation of chloranilic acid to monoanion and dianion with resonance structures shown in brackets.

bonds have similar values of bond lengths and it applies also to four C–O bonds.

The geometries of the anions (Figure 1, Table 2) reported here agree well with results of *ab initio* calculations<sup>19</sup> (Table 2) and data for analogous structures extracted from Cambridge Structural Database.<sup>13</sup> It is

**Figure 1.** ORTEP drawing of chloranilate dianion of *C<sub>i</sub>* crystallographic symmetry in the structure of ammonium chloranilate monohydrate. Thermal ellipsoids are drawn with the 50% probability level.

**Table 2.** Observed and calculated bond lengths in chloranilic acid dianion

Bond	X-ray <sup>(a)</sup>	Calculated <sup>(b)</sup>
C-C delocalised	1.399(7)	1.421
C-C single	1.541(3)	1.561
C-O delocalised	1.249(7)	1.249
C-Cl single	1.740(3)	1.765

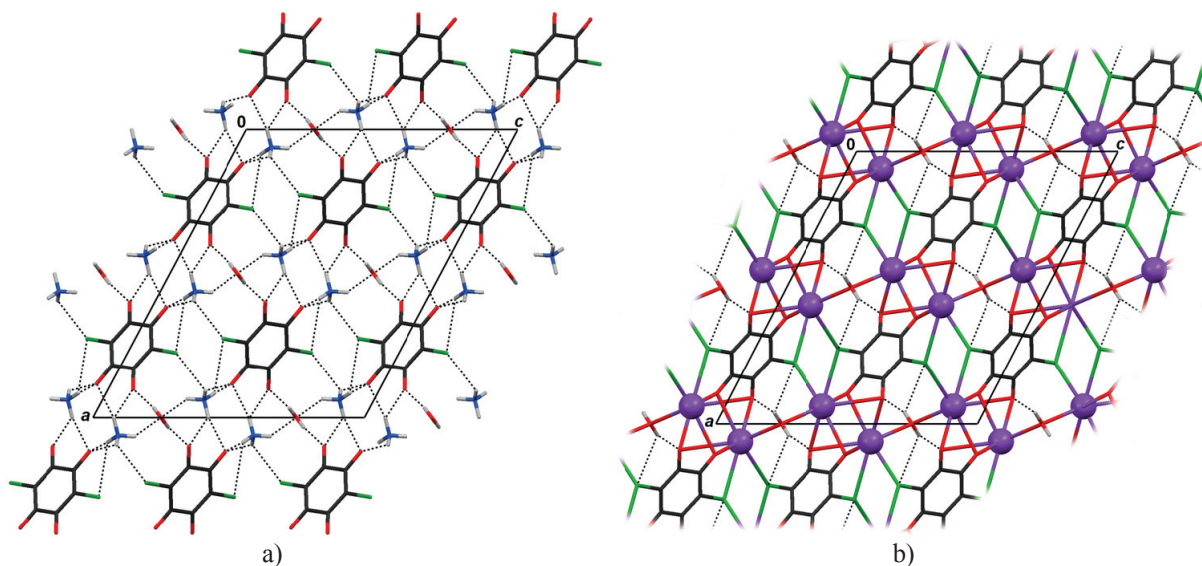
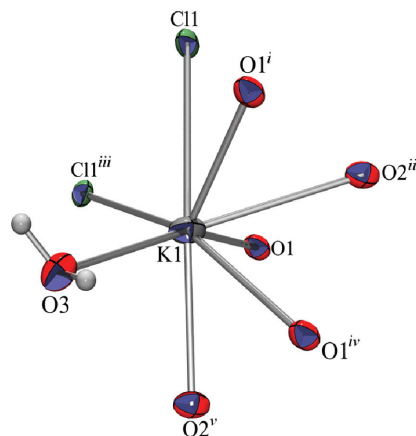
<sup>(a)</sup>Average value of all structures reported in this paper<sup>(b)</sup>MP2 calculations by Ishida & Kashino<sup>19</sup>

observed that the variance of the delocalised bonds is much larger than that of the single bonds (0.007 vs. 0.003 Å). These differences can be assigned to the effect of polarization introduced by hydrogen bonds and alkali ions that are more pronounced on delocalised systems than on localised ones.

### Crystal Packing

Cations in ammonium, potassium and rubidium compounds occupy the same crystallographic positions in the space group *C2/c* (Figure 2). An ammonium cation acts as a donor of four protons, forming seven hydrogen bonds, while the alkali cations are coordinated by eight electron-rich ligands generating distorted coordination polyhedra similar to bicapped octahedra (Figure 3). In the crystals of ammonium chloranilate monohydrate the three-dimensional hydrogen bonded network (Figure 4) is generated *via* eight symmetry-independent hydrogen bonds (including the water molecule) (Table 3).

In the crystal structures of potassium and rubidium chloranilate monohydrates the water molecule acts as a proton donor; it is located on a twofold axis and there is only one symmetry-independent hydrogen bond (Table

**Figure 2.** Crystal packing of a) ammonium chloranilate monohydrate and b) potassium chloranilate monohydrate viewed in the direction [010]. Potassium cations (in violet) are depicted as spheres of arbitrary radii.**Figure 3.** Coordination polyhedron of the potassium cation. Thermal ellipsoids are drawn with the 50 % probability level. Symmetry codes: (i)  $x, 1+y, z$ ; (ii)  $\frac{1}{2}+x, \frac{1}{2}+y, z$ ; (iii)  $\frac{1}{2}-x, \frac{1}{2}+y, \frac{1}{2}-z$ ; (iv)  $1-x, -y, 1-z$ ; (v)  $\frac{1}{2}-x, \frac{1}{2}-y, 1-z$ .

3). Thus, Coulomb oxygen $\cdots$ cation and chlorine $\cdots$ cation interactions dominate in their 3D-network.

In the structure of  $\text{Cs}_{1.5}\text{Na}_{0.5}\text{CA}\cdot\text{H}_2\text{O}$  chloranilate anion is located in the general position; one caesium ion is in the general position, and another one on a twofold axis with the occupancy 0.5. Thus the two different coordinations of the caesium cations occur:  $\text{Cs}^+$  located in a general position is coordinated by eight oxygen atoms disposed at corners of a distorted cube, whereas  $\text{Cs}^+$  in the special position exhibits hepta-coordination (pentagonal bipyramide) surrounded by six oxygen atoms and one chlorine atom.  $\text{Na}^+$  (p.p. = 0.5) located on the twofold axis contributes to the charge balance. Sodium cation has a usual distorted octahedral coordination. The crystal structure of  $\text{Cs}_{1.5}\text{Na}_{0.5}\text{CA}\cdot\text{H}_2\text{O}$  is built of

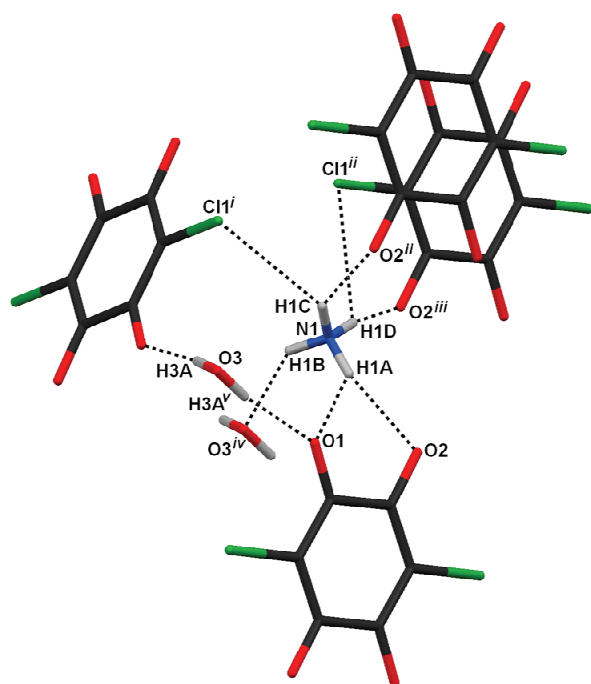


**Figure 4.** The detail in the structure of ammonium chloranilate monohydrate with hydrogen bonding generated by proton donations of ammonium cation. Symmetry codes: (i)  $-\frac{1}{2} + x, -\frac{1}{2} - y, -\frac{1}{2} - z$ ; (ii)  $-x, -1 - y, 1 - z$ ; (iii)  $-x, -y, 1 - z$ ; (iv)  $x, 1 + y, z$ ; (v)  $-x, y, \frac{1}{2} - z$ .

**Table 3.** Geometric parameters of the hydrogen bonds

	$d(\text{D-H}) / \text{Å}$	$d(\text{H}\cdots\text{A}) / \text{Å}$	$d(\text{D}\cdots\text{A}) / \text{Å}$	$\angle(\text{D-H}\cdots\text{A}) / ^\circ$	Symm. op.
$\text{Li}_2\text{CA} \cdot \text{H}_2\text{O}$					
O3-H3A $\cdots$ O1	0.93(4)	1.83(5)	2.685(2)	152(3)	$x, y, 1 + z$
$\text{Na}_2\text{CA} \cdot 2\text{H}_2\text{O}$					
O3-H3A $\cdots$ O1	0.93(2)	2.82(4)	3.210(2)	112(3)	$3/2 - x, -3/2 + y, 1/2 - z$
O3-H3B $\cdots$ Cl1	0.93(3)	2.90(3)	3.247(2)	126(2)	$2 - x, -y, -z$
O3-H3B $\cdots$ O1	0.93(3)	1.95(3)	2.834(2)	159(3)	$1 + x, -1 + y, z$
$\text{K}_2\text{CA} \cdot \text{H}_2\text{O}$					
O3-H3A $\cdots$ O2	0.92(4)	1.96(4)	2.849(3)	163(3)	$\frac{1}{2} + x, -\frac{1}{2} + y, z$
$(\text{NH}_4)_2\text{CA} \cdot \text{H}_2\text{O}$					
N1-H1A $\cdots$ O1	0.92(2)	2.17(3)	2.845(2)	130(2)	$x, y, z$
N1-H1A $\cdots$ O2	0.92(2)	2.11(2)	2.954(2)	151(2)	$x, y, z$
N1-H1B $\cdots$ O3	0.91(3)	2.12(3)	2.896(2)	142(2)	$x, 1 + y, z$
N1-H1C $\cdots$ O2	0.89(2)	2.33(2)	3.081(2)	142(2)	$-x, -1 - y, 1 - z$
N1-H1C $\cdots$ Cl1	0.89(2)	2.79(2)	3.475(2)	135(2)	$-\frac{1}{2} + x, -\frac{1}{2} - y, -\frac{1}{2} + z$
N1-H1D $\cdots$ Cl1	0.91(2)	2.89(3)	3.475(2)	115(2)	$-x, -y, 1 - z$
N1-H1D $\cdots$ O2	0.91(2)	1.90(2)	2.797(2)	168(2)	$-x, -y, 1 - z$
O3-H3A $\cdots$ O1	0.89(2)	1.92(2)	2.084(2)	170(2)	$-x, y, \frac{1}{2} - z$

(continued)

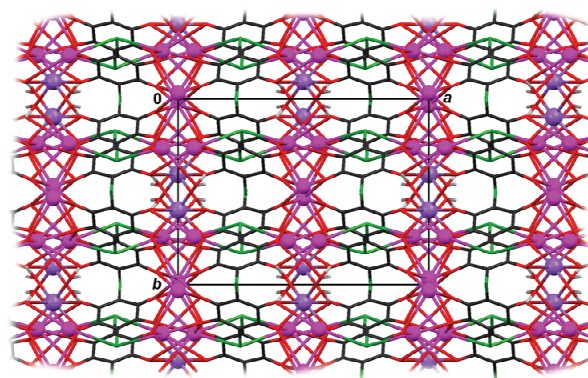


**Figure 5.** Crystal packing of  $\text{Cs}_{15}\text{Na}_{0.5}\text{CA} \cdot \text{H}_2\text{O}$  viewed in the direction [001]. Alkali ions (caesium in pink and sodium in violet) are depicted as spheres of arbitrary radii.

alternating water-cation and anion layers parallel to the (100) plane (Figure 5). Each proton of the water molecule participates in two hydrogen bonds (Table 3). The crystal packing is additionally stabilized by  $\pi \cdots \pi$  stacking interactions between parallel slipped chloranilate anions with centroid-centroid distance of 3.740(2) Å and offset of 1.358 Å. Similar values were observed in the structures of rubidium and caesium hydrogen chloranilate dihydrates [3.587(3) and 3.682(3) Å for Rb-homologue; 3.697(3) and 3.646(2) Å for Cs-homologue with offsets of 1.625 and 1.684 Å; 1.626 and 1.661 Å, respectively].<sup>32</sup>

**Table 3.** Geometric parameters of the hydrogen bonds (continued)

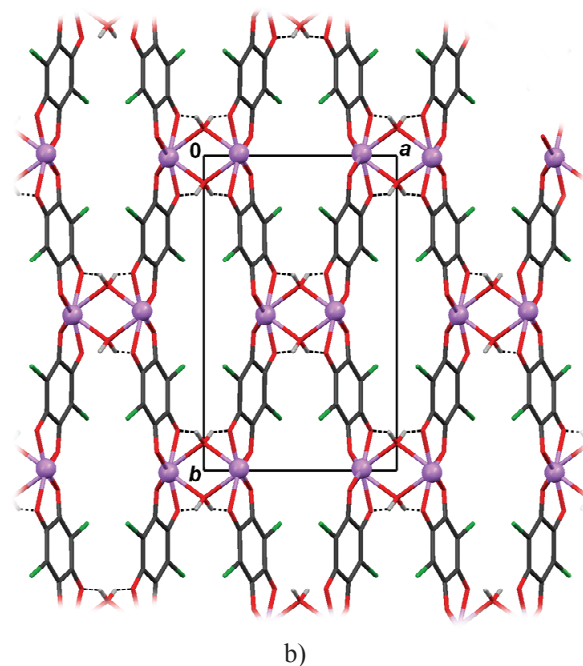
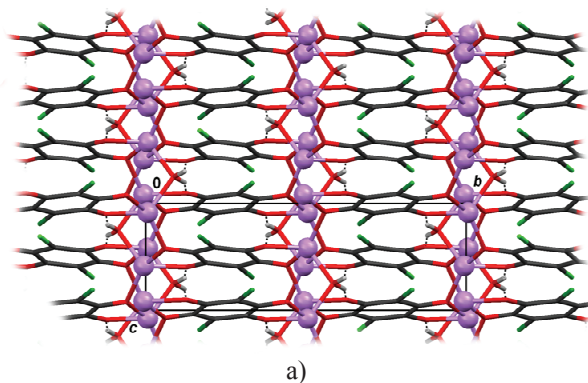
	$d(\text{D-H}) / \text{Å}$	$d(\text{H}\cdots\text{A}) / \text{Å}$	$d(\text{D}\cdots\text{A}) / \text{Å}$	$\angle(\text{D-H}\cdots\text{A}) / ^\circ$	Symm. op.
<b>Rb<sub>2</sub>CA · H<sub>2</sub>O</b>					
O3–H3A···O2	0.91(3)	1.93(3)	2.807(3)	163(3)	$1 - x, -1 + y, \frac{1}{2} - z$
<b>Cs<sub>1.5</sub>Na<sub>0.5</sub>CA · H<sub>2</sub>O</b>					
O5–H5A···Cl1	0.97(6)	2.64(6)	3.537(4)	15 (5)	$\frac{1}{2} + x, \frac{1}{2} + y, z$
O5–H5A···O2	0.97(6)	2.34(6)	3.055(5)	13 (5)	$\frac{1}{2} + x, \frac{1}{2} + y, z$
O5–H5B···Cl2	0.97(5)	2.69(5)	3.391(5)	13 (4)	$1 - x, -y, -z$
O5–H5B···O4	0.97(5)	1.89(5)	2.768(5)	150(4)	$1 - x, -y, -z$

Crystallization from absolute ethanol yielded a novel structure, anhydrous caesium chloranilate (Figure 6) that is substantially different to its hydrate analogue. There are no proton donors in the structure that can create hydrogen bonds with anions. The crystal structure of  $P2_1/c$  symmetry is dominated by Coulomb interactions between closely packed cations and anions ( $D_c = 3.18 \text{ g cm}^{-3}$ ).

The crystal structure of lithium chloranilate monohydrate forms porous, honeycomb-like packing with channels (4.4 Å wide) running in the direction [010] (Figure 7a) and pronounced separation of cation and anion layers parallel to the plane (010) (Figure 7b). Lithium coordination polyhedron is a distorted tetrahedron; double chains of Li-tetrahedra are parallel to the direction [001] (Figure 8). A simple hydrogen bond motif is generated by a single water molecule having two hydrogen atoms related by a twofold axis (Table 3).

The space group and thus the crystal packing of sodium chloranilate dihydrate (Figure 9) is completely different to that of potassium chloranilate monohydrate (Table 1) due to different stoichiometry of the crystal

water molecule. In the sodium structure there is a water molecule in a general position whereas in potassium structure the water molecule occupies the special position (twofold axis). Thus, in the sodium structure there

**Figure 6.** Crystal packing of anhydrous caesium chloranilate viewed in the direction [100]. Caesium cations (in pink) are depicted as spheres of arbitrary radii.**Figure 7.** Crystal packing of lithium chloranilate monohydrate viewed in directions a) [001] and b) [100]. Lithium cations (in violet) are depicted as spheres of arbitrary radii.

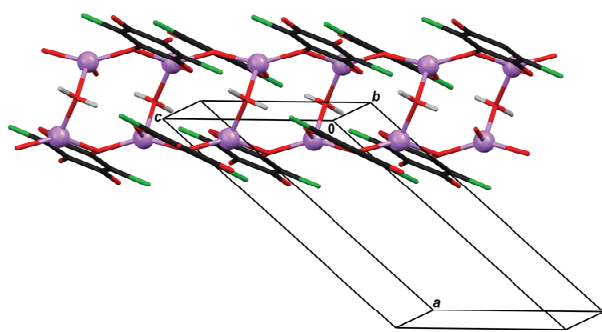


**Figure 8.** Double chains of Li-tetrahedra running parallel to the direction [001]. Lithium cations (in violet) have been depicted as spheres of arbitrary radii.

are two water molecules per chloranilate dianion whereas in potassium there is one. The coordination of sodium cation is a distorted octahedron. Since the water molecule is in a general position, its protons are symmetry-independent: H3A forms very weak hydrogen bond to O1 and H3B acts as double donor to O1 and C11 (Table 3). 3D packing is created by hydrogen bonds and cation...oxygen interactions. The packing interactions also include  $\pi$ ... $\pi$  stacked chloranilate anions with centroid...centroid distance of 3.662(1) Å and offset of 1.698 Å.

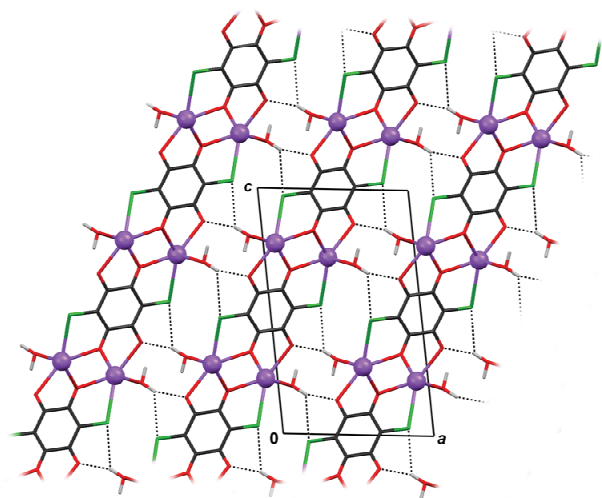


**Figure 9.** Crystal packing of sodium chloranilate dihydrate viewed in the direction [010]. Sodium cations are depicted as spheres of arbitrary radii.

## CONCLUSION REMARKS

The alkali chloranilates described here include three different types of chloranilates: anhydrous compound (caesium chloranilate), monohydrates of potassium, ammonium, rubidium, and caesium<sub>1.5</sub>(sodium<sub>0.5</sub>) chloranilates, and sodium chloranilate dihydrate.

The crystal structures of potassium, ammonium, and rubidium chloranilate monohydrates, all belonging to the space group  $C2/c$ , cannot be isostructural due to intensive hydrogen bonding of the ammonium cation that generates different hydrogen bond network. However, the structures of potassium and rubidium homologues are isostructural.

The most compact packing ( $D_c = 3.183 \text{ g cm}^{-3}$ ) is realised by cation...anion interactions in the structure of anhydrous caesium chloranilate.

The  $\pi$ ...stacked chloranilates which are typical of alkali hydrogen chloranilate dihydrates<sup>32</sup> and *ortho*-chloranilic acid trihydrate<sup>33</sup> also occur in the structures of sodium chloranilate dihydrate and caesium<sub>1.5</sub>(sodium<sub>0.5</sub>) chloranilate monohydrate. However, in the series of compounds described here  $\pi$ ...stacking is not a dominating packing interaction as observed in the crystal packing of hydrogen chloranilates dihydrates.<sup>31</sup> The comparative analysis of the crystal structures with pronounced  $\pi$ ...stacking, having short separation distances [face to face arrangement with separation distance of 3.229(2) Å observed in potassium hydrogen chloranilate dihydrate and 3.335(5) Å in *o*-chloranilic acid trihydrate] and no offset<sup>32,33</sup> and the structures reported here, is in agreement with the observation that hydrogen bonds are predominant factor contributing to attractive polar interactions affecting stacked nonaromatic quinoid rings.

*Supplementary Materials.* – Supplementary crystallographic data for this paper can be obtained free of charge via <http://www.ccdc.cam.ac.uk/conts/retrieving.html> (or from the Cambridge Crystallographic Data Centre, 12, Union Road, Cambridge CB2 1EZ, UK; fax: +44 1223 336033; or deposit@ccdc.cam.ac.uk). CCDC 695072 - 695078 contain the supplementary crystallographic data for this paper.

*Acknowledgements.* This work was supported by Ministry of Science, Education and Sports of Croatia (grant no 098-1191344-2943), Slovenian Research Agency (grant no BI-HR/07-08-025) and grant for the bilateral scientific collaboration between Croatia and Slovenia.

## REFERENCES

1. T. Bountis (Ed.), *Proton Transfer in Hydrogen Bonded Systems*, Plenum Press, New York, 1992.
2. T. Elsaesser, *Coherent Low-frequency Motions in Condensed Phase Hydrogen Bond and Transfer*, in: J. T. Hynes, J. P. Kliman, H.-H. Limbach, and R. L. Schowen (Eds.), *Hydrogen-Transfer Reactions*, Vol. 1, Wiley-VCH, New York, 2007, pp. 459–479.
3. T. Kojima, K. Nakagawa, and Z. Shiegetomi, *Anal. Sci.* **10** (1994) 939–942.
4. J. Ramkumar, *Talanta* **68** (2006) 902–907.
5. M. Flores, R. Isaacson, E. Abresch, R. Calvo, W. Lubity, and G.

- Feher, *Biophys. J.* **92** (2007) 671–682.
6. M. Aguilar-Martinez, N. A. Macias-Ruvalcaba, J. A. Bautista-Martinez, M. Gómez, F. J. González, and L. González, *Curr. Org. Chem.* **8** (2004) 1721–1738.
  7. P. J. O'Malley, *Antioxid. Redox Signaling* **3** (2001) 825–837.
  8. M. P. Bernstein, S. A. Sandorf, L. J. Alamandolla, J. S. Gillette, S. J. Clemett, and R. N. Zare, *Science* **283** (1999) 1135–1138.
  9. H. Sies and L. Packer (Eds.), *Methods in Enzymology: Quinones and Quinone Enzymes*, Part B, Vol. 382, Academic Press, London, 2004.
  10. Y. Fu, L. Buryanovsky, and Z. Zhang, *Biochem. Biophys. Res. Commun.* **336** (2005) 332–338.
  11. R. York and M. R. Marshall, *J. Food Biochem.* **27** (2003) 361–422.
  12. S. Bittner, *Amino Acids* **30** (2006) 205–224.
  13. F. H. Allen, *Acta Crystallogr., Sect. B* **58** (2002) 380–388.
  14. E. K. Andersen, *Acta Crystallogr.* **22** (1967) 196–201.
  15. F. H. Herebstein and M. Kaftory, *J. Appl. Crystallogr.* **5** (1972) 51–52.
  16. S. Kitagawa and S. Kawata, *Coord. Chem. Rev.* **224** (2002) 11–34.
  17. B. F. Abrahams, J. Coleiro, K. Ha, B. F. Hoskins, and S. D. Orchard, *J. Chem. Soc., Dalton Trans.* (2002) 1586–1594.
  18. P. Gupta, A. Das, F. Basuli, A. Castineiras, W. S. Sheldrick, H. Mayer-Figge, and S. Bhattacharya, *Inorg. Chem.* **44** (2005) 2081–2088.
  19. H. Ishida, S. Kashino, *Z. Naturforsch., A* **57** (2002) 829–836.
  20. H. Ishida, *Acta Crystallogr., Sect. E* **60** (2004) o974–o976.
  21. K. Gotoh, T. Asaji, and H. Ishida, *Acta Crystallogr., Sect. C* **63** (2007) o17–o20.
  22. O. Kühl and S. Gouta, *Cryst. Growth Des.* **5** (No 5) (2005) 1875–1879.
  23. M. Dworniczak, *React. Kinet. Catal. Lett.* **78** (2003) 65–72.
  24. K. S. Min, A. G. DiPasquale, J. A. Golen, A. L. Rheingold, and J. S. Miller, *J. Am. Chem. Soc.* **129** (2007) 2360–2368.
  25. K. Molčanov, B. Kojić-Prodić, and M. Roboz, *Acta Crystallogr., Sect. B* **62** (2006) 1051–1060.
  26. T. Nihei, S. Ishimaru, H. Ishida, H. Ishihara, and R. Ikeda, *Chem. Phys. Lett.* **329** (2000) 7–14.
  27. S. Horiuchi, R. Kumai, and Y. Tokura, *Chem. Commun.* (2007) 2321–2329.
  28. R. Kumai, S. Horiuchi, Y. Okimoto, and Y. Tokura, *J. Chem. Phys.* **125** (2006) 084715.
  29. S. Kitagawa, R. Kitaura, and S. Noro, *Angew. Chem., Int. Ed.* **43** (2004) 2334–2375.
  30. S. Kitagawa and R. Matsuda, *Coord. Chem. Rev.* **251** (2007) 2490–2509.
  31. S. Horiike, R. Matsuda, D. Tanaka, S. Matsubara, M. Mitzuno, K. Endo, and S. Kitagawa, *Angew. Chem., Int. Ed.* **45** (2006) 7226–7230.
  32. K. Molčanov, B. Kojić-Prodić, and A. Meden, *CrystEngComm* (2009), DOI: 10.1039/b821011j.
  33. J. Stare, K. Molčanov, S. Kazazić, B. Kojić-Prodić, to be submitted to *Acta Crystallogr., Sect. B*.
  34. L. Vanino (Ed.), *Handbuch der synthetischen Chemie*, F. Enke Verlag, Stuttgart, 1937.
  35. K. Harms and S. Wocadlo, (1995) XCAD-4. Program for Processing CAD-4 Diffractometer Data. University of Marburg, Germany.
  36. CrysAlis PRO, Oxford Diffraction Ltd., Version 1.18 (2008).
  37. Z. Otwinowski and W. Minor, *Methods Enzymol.* **276** (1997) 307–326.
  38. G. M. Sheldrick, *Acta Crystallogr., Sect. A* **64** (2008) 112–122.
  39. T. Spek, PLATON98: *A Multipurpose Crystallographic Tool*, 120398 Version, University of Utrecht, Utrecht, The Netherlands, 1998.
  40. L. J. Farrugia, ORTEP-3 for Windows, *J. Appl. Crystallogr.* **30** (1997) 565–565.
  41. C. F. Macrae, P. R. Edgington, P. McCabe, E. Pidcock, G. P. Shields, R. Taylor, M. Towler, J. Van der Streek, *J. Appl. Crystallogr.* **39** (2006) 4563–457.
  42. R. Benchekrroun and J.-M. Savariault, *Acta Crystallogr., Sect. C* **51** (1995) 186–188.

## SAŽETAK

### Jedinstvena elektronska i strukturna svojstva 1,4-benzokinonâ: kristalokemija hidratâ alkalijskih kloranilata

Krešimir Molčanov,<sup>a</sup> Biserka Kojić-Prodić<sup>a</sup> i Anton Meden<sup>b</sup>

<sup>a</sup>Institut Ruđer Bošković, p. p. 180, 10002 Zagreb, Hrvatska

<sup>b</sup>Faculty of Chemistry and Chemical Technology, University of Ljubljana, Slovenia

Zahvaljujući jedinstvenim elektronskim i strukturnim karakteristikama 1,4-benzokinona, ti spojevi ostvaruju mnogobrojne interakcije, poput koordinacijske veze, vodikovih veza s prijenosom protona i/ili elektrona,  $\pi$ -interakcije te redoks-aktivnosti, koje priroda koristi u važnim biološkim reakcijama. Unatoč širokoj uporabi u supramolekularnoj kemiji i pripravi funkcionalnih materijala, međusobni utjecaj različitih interakcija nije sasvim istražen. Utjecaj vodikovih veza i kationâ na interakcije, koje tvori kinoidni prsten proučavane su na seriji hidratâ alkalijskih ( $\text{Li}^+$ ,  $\text{Na}^+$ ,  $\text{K}^+$ ,  $\text{NH}_4^+$ , i  $\text{Rb}^+$ ) kloranilata te bezvodnoga cezijeva kloranilata. U struktura natrijeva kloranilata dihidrata i cezijeva natrijeva kloranilata monohidrata  $\pi\cdots\pi$  interakcije određuju slaganje kloranilatnih dianionâ, [udaljenosti između centroidâ prstenova su 3.662(1) i 3.740(2) Å, a posmaci 1.698 and 1.358 Å]; te interakcije modulirane su vodikovim vezama preko molekula kristalne vode. Kristalne strukture kalijeva i rubidijeva kloranilata monohidrata su izostrukturalne, dok amonijev homolog ima posve drugačiju mrežu vodikovih veza jer je kation jaki donor protona. U šest od sedam opisanih struktura kloranilatâ dianion ima kristalografsku simetriju  $C_i$ .